

Multimodal Fluorescence Switching Materials: One Dye to Have Them All

Jaume Ramon Otaegui, Aleix Carrascull-Marín, Daniel Ruiz-Molina, Jordi Hernando,* and Claudio Roscini*

Off/on, on/off, and on₁/on₂ fluorescence switching systems find application in a variety of areas, for each of which a particular dye or dye-switch tether must be specifically designed and synthesized. Herein it is demonstrated that such tight requirement can be avoided by using easily prepared mixtures of readily available emitters and phase change materials (PCMs). By proper selection of the PCM and, if needed, additives, thermo- and photothermoreponsive materials showing all classes of emission switching modes can be prepared from a single dye and without chemical modifications. This strategy can be generalized to distinct emitters and, thanks to the facile and versatile printability of dye-PCM mixtures, it can be used for the fabrication of fluorescent patterns showing complex (photo)thermal responses with direct applicability in sensing and anti-counterfeiting.

single-color off-on and on-off fluorescent switches interconvert between emissive and nonemissive states. Among them, off-on systems are preferred for optical sensing,^[11,23,24] as higher sensitivities can be reached by detecting tiny fluorescence signals above a dark background. On the contrary, on-off switches are exploited in super-resolution fluorescence microscopy, which typically requires reversibly extinguishing the emission of fluorophores either in time (in coordinate-stochastic methods)^[25,26] or space (in coordinate-targeted methods).^[27,28] On the other hand, dual-color fluorescent switches are designed to toggle between two differently colored emissive states (on₁-on₂),^[17] a behavior

that offers several advantages for sensing and anti-counterfeiting applications (e.g., reduced interference from the autofluorescence of the medium,^[22] quantitative ratiometric measurements,^[22,29] and multiple readout modes for higher security levels^[18,20]).

In all these systems fluorescence modulation is normally accomplished through switchable molecules that, when subjected to an external stimulus, either show intrinsic interconversion between distinct emissive states or differently interact with nearby fluorescent dyes.^[22,30] Therefore, in order to vary the switching scheme, different inherently fluorescent switching or multicomponent molecules must be designed and synthesized on a case-by-case basis, which hampers their general implementation. Thus, the development of a universal approach to accomplish multiple emission switching behaviors using the same dye has become a long-sought mission.

Herein we hypothesize that this challenge can be reached reversing the underlying design criterion, that is, by modulation of the environment or matrix, while fixing a fluorescent dye with multiple emissive responses. To demonstrate this premise, we chose phase change materials (PCMs) as matrices, whose (photo)thermally-triggered solid-to-liquid transition has been recently proven to modulate the fluorescence of the dissolved emitters thanks to changes of medium rigidity or dye aggregation state.^[11,31–40] As for the dye, we must select molecular emitters that, under controlled modification of the surrounding environment, are capable of undergoing both single- and two-color fluorescence switching through different photochemical mechanisms. For instance, this is the case of the perylene

1. Introduction

Switchable fluorescent materials are receiving much attention from both the academic and industrial sectors due to their broad applicability in a wide range of areas,^[1–6] which span from optical memories^[7,8] and logic gates^[9] to (bio) sensing^[10–14] and bioimaging probes,^[15–17] and anti-counterfeiting technologies.^[18–21] Different fluorescent switching modes are available for these materials, each of which is best suited for particular applications.^[22] On the one hand,

J. R. Otaegui, A. Carrascull-Marín, C. Roscini
Nanostructured Functional Materials
Catalan Institute of Nanoscience and Nanotechnology (ICN2)
CSIC and BIST
Campus UAB, Bellaterra, Barcelona 08193, Spain
E-mail: claudio.roscini@icn2.cat

J. R. Otaegui, D. Ruiz-Molina, J. Hernando
Departament de Química
Universitat Autònoma de Barcelona
Edifici C/n, Campus UAB, Cerdanyola del Vallès 08193, Spain
E-mail: jordi.hernando@uab.cat

 The ORCID identification number(s) for the author(s) of this article can be found under <https://doi.org/10.1002/adom.202200083>.

© 2022 The Authors. Advanced Optical Materials published by Wiley-VCH GmbH. This is an open access article under the terms of the Creative Commons Attribution-NonCommercial License, which permits use, distribution and reproduction in any medium, provided the original work is properly cited and is not used for commercial purposes.

DOI: 10.1002/adom.202200083

diimide derivative *N,N'*-bis(1-hexylheptyl)perylene-3,4,9,10-bis(dicarboximide) (PDI, Figure S1, Supporting Information), a bright and stable lime green fluorophore in diluted organic solutions whose emission can be i) switched off by photoinduced electron transfer (PET) in the presence of close-by electron donors,^[41,42] and ii) turned into red excimer luminescence upon aggregation in concentrated mixtures^[41] or polymer media.^[43] Therefore, the use of PCMs to modulate the behavior of this class of dyes offers a unique and straightforward approach toward photo- and thermofluorochromic materials that exhibit multiple switching modes.

2. Results and Discussion

To validate our strategy, we first aimed to obtain dual-color on₁/on₂ switching using PDI-PCM mixtures. For this, we employed a 0.1 wt.% solution of PDI in eicosane (EC, $T_m^{EC} = 37\text{ °C}$ ^[44]), a 20-carbon paraffin that has already been used to interconvert between the monomer and aggregation-induced excimer fluorescence of polycyclic aromatic dyes upon thermally-induced solid-liquid phase transition.^[32,34] This is due to the fact that these dyes dissolve well in the liquid paraffin, while they aggregate in the solid phase because of lower solubility (Figure 1a

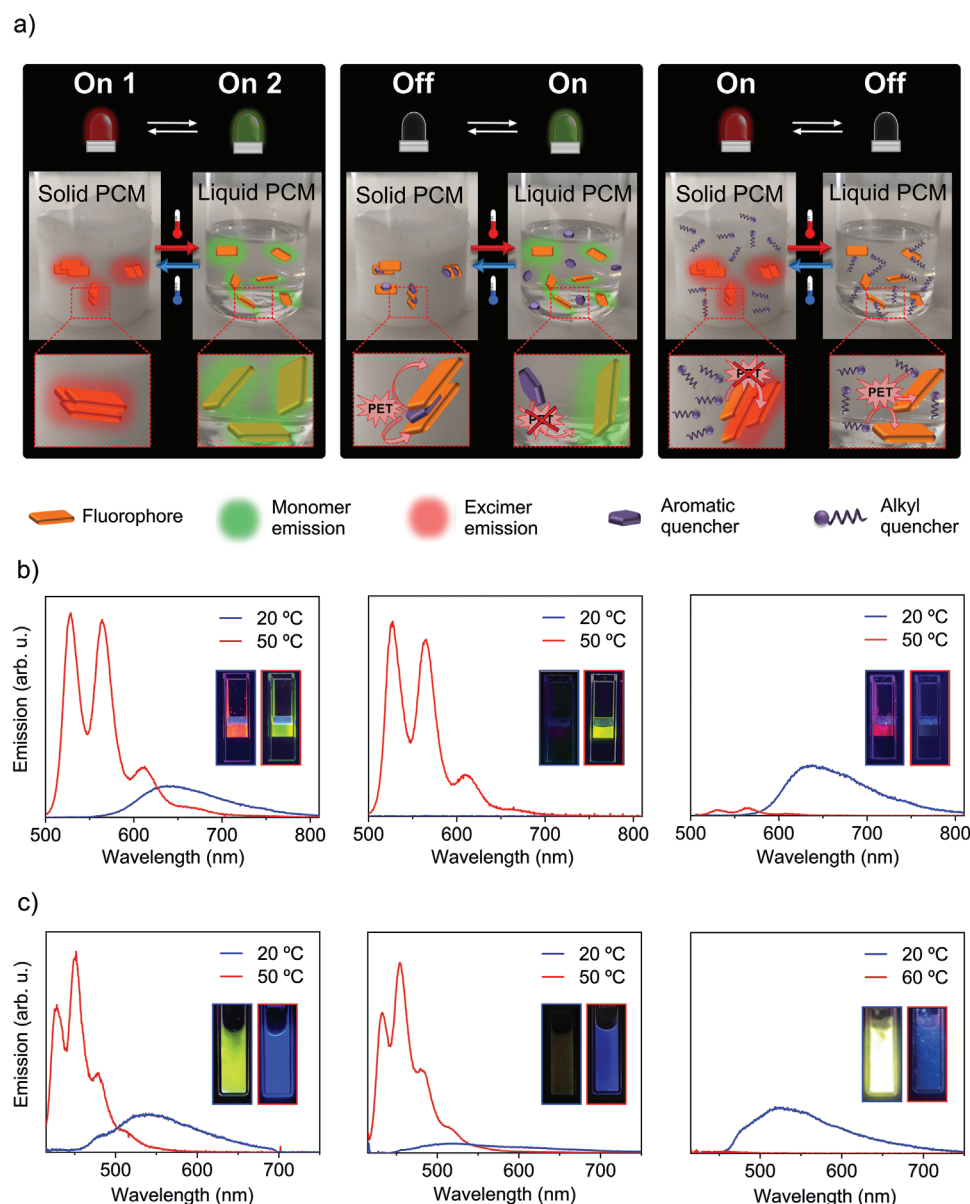


Figure 1. a) Schematic representation of the distinct fluorescence switching behaviors accomplished by varying the nature of the PCM and/or the incorporation of additives: on₁-on₂ modulation by interconverting between excimer and monomer dye emission; off-on modulation by adding a PET quencher as an additive; on-off modulation by using the PCM matrix as a PET quencher. b) Emission spectra of PDI-loaded PCM mixtures in the solid (blue) and liquid (red) state ($\lambda_{exc} = 445\text{ nm}$): PDI@EC (on₁-on₂, $c_{PDI} = 0.1\text{ wt.}\%$), PDI-DBA@EC (off-on, $c_{PDI} = 0.1\text{ wt.}\%$, $c_{DBA} = 0.005\text{ wt.}\%$), and PDI@EC-OAME (on-off, $c_{PDI} = 0.5\text{ wt.}\%$, 7:3 EC:OAME). c) Emission spectra of DCA-loaded PCM mixtures in the solid (blue) and liquid (red) state ($\lambda_{exc} = 405\text{ nm}$): DCA@EC (on₁-on₂, $c_{DCA} = 0.007\text{ wt.}\%$), DCA-DMA@EC (off-on, $c_{DCA} = 0.007\text{ wt.}\%$, $c_{DMA} = 0.17\text{ wt.}\%$) and DCA@OA (on-off, $c_{DCA} = 0.007\text{ wt.}\%$).

and Figure S2a, Supporting Information). As anticipated, the solid PDI@EC mixture displayed the typical red and broad excimer-like emission of this dye with rather high quantum yield (on_1 , $\lambda_{\text{max}} = 640 \text{ nm}$, $\Phi_f = 0.40$), which turned into the bright, lime green and structured fluorescence characteristic of PDI monomers upon thermally melting the sample (on_2 , $\lambda_{\text{max}} = 528 \text{ nm}$, $\Phi_f = 0.89$) (Figure 1b). Such emission measured in the liquid state is slightly altered and less intense than expected for diluted PDI solutions ($\Phi_f \approx 1$ in most organic solvents^[41]), which we attribute to self-absorption processes occurring at the higher dye concentrations employed.

Off/on thermofluorochromism was accomplished by dissolving PDI in EC (0.1 wt.%), though in the presence of the electron donor *N,N*-dibutylaniline as an additive (DBA, 0.005 wt.%). Because of its aromatic core, DBA should aggregate together with PDI molecules in solid EC, and thus promote efficient emission quenching by PET (Figure 1a). In fact, nearly no fluorescence was measured for the PDI-DBA@EC mixture in its solid-state (off, $\Phi_f = 0.035$). In contrast, when the sample was heated above T_m^{EC} , the intense PDI monomer emission was registered owing to the dissolution of the heteroaggregates of PDI and DBA molecules, which barely interact in the liquid PCM at the low concentrations used (on , $\lambda_{\text{max}} = 528 \text{ nm}$, $\Phi_f = 0.81$) (Figure 1b and Figures S2b–S3, Supporting Information).

Finally, to realize thermoresponsive on/off fluorescence switching, the use of a different PCM that not only triggers selective PDI aggregation but is also sufficiently electron-donating as to induce PET-based emission quenching was tested. Under such circumstances, the red excimer fluorescence from the large PDI homoaggregates formed in the solid-state is expected to be mainly preserved, as only the minor fraction of dyes located at (or close to) the outer surface of the aggregates should undergo PET processes with the enclosing PCM matrix. However, redissolution of the aggregates upon thermally melting the mixture should make all PDI emitters be surrounded by the large excess of PCM molecules, which must completely quench the fluorescence of the sample in its liquid state by PET (Figure 1a).

To test this hypothesis, we first dissolved PDI in pure *N*-methyloctadecylamine (OAME, 0.1 wt.%, $T_m^{\text{OAME}} = 52.9 \text{ }^\circ\text{C}$ ^[44]). Although the resulting PDI@OAME mixture exhibited on/off thermofluorochromism, a rather poor emission efficiency was registered for the solid-state of the sample ($\Phi_f = 0.03$), probably due to the small size of the PDI aggregates formed (i.e., the short distances between the inner dyes and the aggregates' surface) and/or the large amount of surrounding OAME quenching sites. Accordingly, we decided to i) use mixtures of OAME with a nonquenching PCM (EC) as a host, and ii) raise PDI concentration to increase dye aggregates' size. After evaluating the variation of PDI emission quantum yield when dispersed in solid and melted EC-OAME matrices of variable composition, the best results were obtained for a 7:3 EC-OAME mass ratio and a 0.5 wt.% dye concentration (Figures S2c and S4, Supporting Information). At these conditions PDI@EC-OAME shows strong red excimer fluorescence in the solid-state (on , $\lambda_{\text{max}} = 642 \text{ nm}$, $\Phi_f = 0.19$) and negligible lime green monomer emission upon melting (off, $\Phi_f = 0.010$) (Figure 1b).

All the three emission switching modes registered for PDI@EC, PDI-DBA@EC, and PDI@EC-OAME mixtures were found to be fully reversible, as the initial luminescence of the solid samples was retrieved upon cooling their melts and even after applying several heating-cooling cycles (Figure S5, Supporting Information). In addition, their behavior was demonstrated to be generalizable to other emitters that also sustain multiple fluorescence modulation mechanisms (e.g., excimer formation upon aggregation and PET-induced quenching). For this, we chose the dye 1,6-dicyanoanthracene (DCA, Figure S1, Supporting Information). After some optimization work required because of the different chemical nature of DCA, we observed that, by dissolving this dye in pristine eicosane (DCA@EC, 0.007 wt.%), in eicosane together with *N,N*-dimethylaniline (DMA, 0.17 wt.%) (DCA-DMA@EC, 0.007 wt.%), and in octadecylamine (OA) (DCA@OA, 0.007 wt.%), the resulting mixtures exhibited on_1/on_2 , off/on and on/off emission modulation schemes, respectively (Figure 1c). Noticeably, both the monomer and excimer emissions of DCA in these samples are blue-shifted with respect to those made from PDI, thus allowing the three switching modes to occur in different spectral regions.

Prompted by these successful results, we aimed to exploit our PCM-based strategy for the fabrication of different solid materials of interest for practical applications. First, we prepared thermally-responsive smart papers by soaking cellulose substrates with the PDI- and DCA-loaded mixtures described above. The soaked papers fully preserved all the optical switching modes of the corresponding bulk mixtures (Figure 2 and Figure S6, Supporting Information). However, it must be noted that larger amounts of the quenching amines DBA and DMA had to be used to reproduce the bulk off/on fluorescence behavior in the impregnated substrates ($c_{\text{amine}} \approx 0.20\text{--}0.25 \text{ wt.}\%$). We attribute this result to the migration of the amine molecules towards the cellulose fibers, thus decreasing their concentration in the PCM phase. Actually, this process was found to occur even after preparation of the samples, as the amine quenching effect in the solid-state of the material strongly decreased after storage at room temperature for several days and irrespective of the surrounding atmosphere (air or inert atmosphere), which discarded the loss of the amine due to oxidation. By contrast, when slowing down molecular diffusion by storing the substrates at $4 \text{ }^\circ\text{C}$, their emission off/on modulation was preserved after at least 1 week.

In addition, when the cellulose papers soaked with dye-PCM mixtures were also impregnated with an aqueous dispersion of gold nanoshells (diameter = $96 \pm 34 \text{ nm}$, Figure S7, Supporting Information), they underwent localized on_1/on_2 , off/on and on/off fluorescence switching upon irradiation with a near-infrared (NIR) laser ($\lambda_{\text{exc}} = 830 \text{ nm}$, Figure 2 and Figure S6, Supporting Information). As previously reported by us,^[31] this effect results from the photothermal heating generated by the gold nanoshells, which induces the melting of the dye-PCM phase and, as a result, the modulation of emission selectively in the illuminated area. Importantly, the same behavior could be accomplished when replacing the gold nanoshells with solid gold nanoparticles (diameter = $18 \pm 5 \text{ nm}$, Figure S8, Supporting Information) and using green excitation light to induce photothermal heating instead ($\lambda_{\text{exc}} = 532 \text{ nm}$, Figure S9, Supporting Information). Therefore, this demonstrates that the

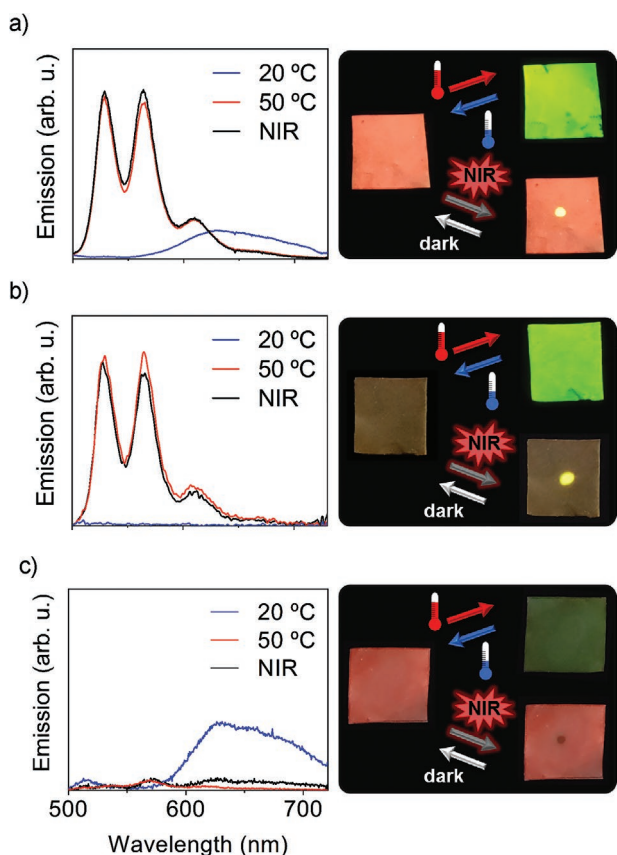


Figure 2. Emission spectra (left, $\lambda_{\text{exc}} = 355$ nm) and images (right, $\lambda_{\text{exc}} = 365$ nm) of cellulose papers soaked with a) PDI@EC, b) PDI-DBA@EC, and c) PDI@EC-OAMe at room temperature in the dark, when heated above T_m^{PCM} and when locally irradiated with a NIR laser ($\lambda_{\text{exc}} = 830$ nm).

conditions required to obtain local light-induced fluorescence modulation in dye-PCM mixtures can be easily tuned by varying the nature and excitation spectra of the photothermal nanoheaters employed.

For the cellulose substrates impregnated with dye-PCM mixtures, we further analyzed the performance of the local emission changes achieved optically. First, we investigated the spatial resolution with which these changes can be induced. With this aim, we conducted fluorescence microscopy experiments where a soaked paper was excited with a focused NIR laser beam ($\lambda_{\text{exc}} = 980$ nm, spot = $1000 \times 300 \mu\text{m}^2$) while monitoring its fluorescence over a larger field of view (Figure S10, Supporting Information). For PDI@EC samples, photothermally-triggered red-to-green fluorescence switching was observed to occur within a region of the substrate that is much larger than the excitation spot ($>1400 \times 1400 \mu\text{m}^2$, Figure S10, Supporting Information). This is due to the thermal gradient created, which spreads the photothermal heat outside of the illuminated area and promotes PCM melting in the surrounding region because of the low T_m of EC ($T_m^{\text{EC}} = 37$ °C^[44]). Though this result could be slightly improved by decreasing the excitation power and the concentration of photothermal nanoheaters, the best spatial resolution was accomplished when selecting PCMs of higher melting points; that is, when disfavoring PCM melting in the areas surrounding the illuminated spot through

photothermal heat diffusion. Thus, when the same experiment was performed for a cellulose paper impregnated with a PDI-octacosane mixture (OC, $T_m^{\text{OC}} = 60$ °C^[44]), we were not only able to retrieve the on₁-on₂ fluorescence switching previously observed for PDI@EC, but in this case, the local red-to-green emission change could be essentially restricted to the photoexcited area (Figure S10, Supporting Information). Consequently, wise selection of the sample components and illumination conditions should enable high spatial resolution of the local fluorescence modulation attained in dye-PCM mixtures.

Moreover, we also investigated the kinetics of the photoactivated fluorescence changes locally induced in soaked cellulose papers. It must be noted that such kinetics is not only dependent on the rate with which the PCM is photothermally melted in the illuminated area, but also on the time that it takes the local heat generated to diffuse to other regions of the sample and the surrounding environment until a thermostationary state is created. Overall, this means that a number of parameters should affect the actual switching kinetics observed; for example, the PCM melting temperature, the photoexcitation power and photothermal nanoheater concentration determining the heating rate, the dimensions of the heated volume, the room temperature, and the heat conductivity of the material. As a result, large variability of the emission switching times could be observed. For instance, for papers impregnated with low- T_m mixtures PDI@EC, PDI-DBA@EC, and PDI@EC-OAMe, emission switching could be appreciated almost immediately when photothermally heated with a non-focused NIR laser, though constant fluorescence modulation was not observed until illumination for tens of seconds (Figure S11, Supporting Information). Actually, such very fast activation of the fluorescence changes could be clearly observed by fluorescence microscopy for substrates soaked with both low- T_m PDI@EC and high- T_m PDI@OC mixtures (Figure S12, Supporting Information), which permits real-time handwriting of fluorescent patterns on the papers (Movie S1, Supporting Information).

Aside from continuously coated cellulose supports, we also investigated the deposition of our PCM mixtures on different substrates as stimuli-responsive fluorochromic patterns, as described for smart papers inkjet-printed with gold nanoshells^[31] or nanostructured dye-loaded paraffin mixtures.^[32] Herein we instead fabricated thermofluorochromic patterns by means of spray coating, a much more versatile technique that allows depositing such thermofluorochromic mixtures onto substrates other than cellulose papers. However, this approach requires previous microstructuring of the PDI-loaded PCMs as solid lipid microparticles (SLMs), which we achieved through an oil-in-water emulsion cooling method. In this method, the oil droplets were obtained by homogenizing the molten PDI-PCM mixture in a hot surfactant-containing aqueous phase, which was then rapidly cooled down to obtain the desired SLMs (see the Supporting Information for further details). Optical microscopy measurements corroborated the successful formation of microparticles with 15–21 μm in diameter (Figure S13, Supporting Information), while ¹H NMR spectroscopy confirmed the encapsulation of the amines required for accomplishing off/on (DBA) and on/off (OAMe) fluorescence modulation (Figures S14 and S15, Supporting Information).

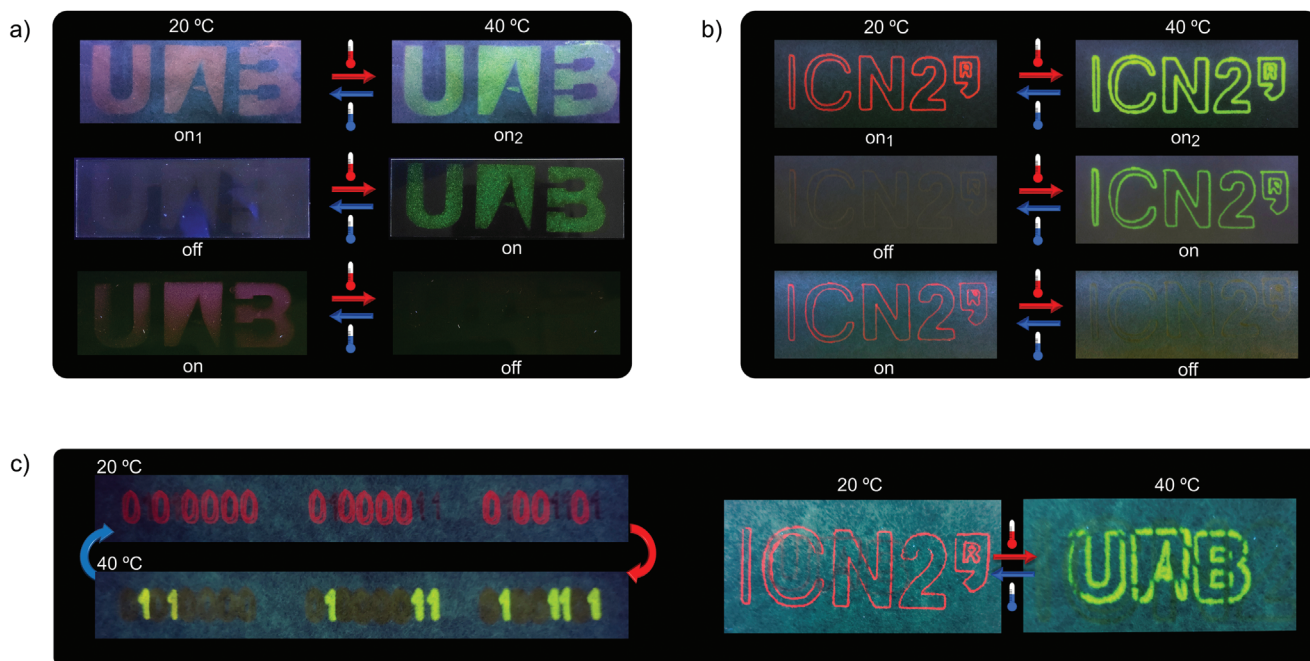


Figure 3. a) Images of thermofluorochromic patterns prepared from PDI@EC_SLMs (top), PDI-DBA@EC_SLMs (middle), PDI@EC-OAMe_SLMs (bottom) spray-coated onto cellulose paper, glass and polystyrene substrates, respectively. b) Images of thermofluorochromic patterns prepared from PDI@EC (top), PDI-DBA@EC (middle), and PDI@EC-OAMe (bottom) printed onto cellulose with a custom-made plotter. c) Wax-printed patterns obtained depositing on/off (PDI-DBA@EC) and off/on (PDI@EC-OAMe) fluorescence switching dye-PCM mixtures in different (left) or the same (right) area of the cellulose paper. All images are taken under UV light (365 nm).

The microparticle suspensions obtained for the three different PDI-loaded mixtures (PDI@EC_SLMs, PDI-DBA@EC_SLMs, PDI@EC-OAMe_SLMs) could be successfully spray-coated onto different substrates (porous cellulose papers, flat glass, and a polystyrene film, Figure S16, Supporting Information), for which we used a customized spray-dryer and a pre-patterned poly(methyl methacrylate) mask (Figure S17, Supporting Information). As shown in Figure 3a and Figure S18a, Supporting Information, all printed materials preserved the switching properties of the respective bulk mixtures and maintained the pattern resolution even after various heating/cooling cycles.

In addition, we also explored the patterning of dye-PCM mixtures using wax-printing, a rather simple method that does not require prior PCM structuration. This was accomplished by using a custom-made plotter where a pen was loaded with the desired PDI-PCM mixture, coated with metallic foil connected to a power supply to induce PCM melting by Joule heating, and attached to a drawing robot with 3D motion that allows reproducing pre-designed patterns (Figure S19, Supporting Information). In this way, complex marks could be printed onto paper, which retained the reversible thermofluorochromic switching behavior of the bulk samples and did not smear out upon sequential heating/cooling cycles (Figure 3b, Figure S18b and Movie S2, Supporting Information). On top of that, we could also use wax-printing for sequentially depositing on/off (PDI-DBA@EC) and off/on (PDI@EC-OAMe) PDI-loaded PCM mixtures on different or even the same region of cellulose substrates (Figure 3c). In this way, materials were obtained that show dual-color thermofluorochromic transition between two

different patterns, a very appealing feature for high-security anti-counterfeiting applications that normally is only possible with the use of electronic digital devices.

Taking advantage of the simplicity of the wax-printing process, we also demonstrated the potential of our dye-PCM mixtures to be used as thermal sensors. For this, we printed three off/on thermofluorochromic patterns that exhibit distinct activation temperatures on the external surface of a disposal paper cup: $T_m^{EC} = 37\text{ }^\circ\text{C}^{[44]}$ for the already described PDI-DBA@EC mixture and $T_m^{TC} = 51\text{ }^\circ\text{C}^{[44]}$ and $T_m^{OC} = 60\text{ }^\circ\text{C}^{[44]}$ for the analogous samples with the higher- T_m PCMs tetracosane (PDI-DBA@TC) and octacosane (PDI-DBA@OC), respectively. As shown in Figure S20, Supporting Information, the change in the fluorescence emission from these patterns clearly report on the temperature of the liquid inside the cup when it varies from 14 to 65 °C.

In summary, herein we demonstrate that, by dispersing a selected dye in adequate PCMs, thermofluorochromic systems are obtained that exhibit all the possible types of emission switching schemes (on₁-on₂, off-on, on-off) without the need for synthetic modification of the emitter. Moreover, thanks to the versatility of the resulting dye-PCM mixtures, smart responsive papers were obtained by simply soaking them into the desired mixture, and even more sophisticated thermally-responsive patterns were created with facile printing technologies. These results pave the way for the fabrication of luminescent smart materials showing intricate stimuli-responsive behavior as highly attractive platforms for the development of optical sensors and anti-counterfeiting technologies at very reduced cost and effort.

Supporting Information

Supporting Information is available from the Wiley Online Library or from the author.

Acknowledgements

This work was supported by grant RT12018-098027-B-C21 and PID2019-106171RB-I00 funded by MCIN/AEI/10.13039/501100011033 and by ERDF – “A way of making Europe”. The ICN2 is funded by the CERCA program/Generalitat de Catalunya and supported by the Severo Ochoa “Centers of Excellence” program, grant SEV-2017-0706 funded by MCIN/AEI/10.13039/501100011033. U.A.B. thanks the support from Generalitat de Catalunya (2017 SGR00465 project). J.R.O. thanks the Generalitat de Catalunya (AGAUR) for his predoctoral FI fellowship. The authors acknowledge the Research Support Division – Instrumentation Unit of ICN2 for the help in the instrumentation design.

Conflict of Interest

The authors declare no conflict of interest.

Data Availability Statement

Research data are not shared.

Keywords

dual-color switch, fluorescence, phase change materials, single-color switch, solid lipid particles

Received: January 14, 2022
Revised: May 19, 2022
Published online:

- [1] E. Yildiz, F. M. Deniz, Raymo, *Chem. Soc. Rev.* **2009**, *38*, 1859.
- [2] D. Bléger, S. Hecht, *Angew. Chem., Int. Ed.* **2015**, *54*, 11338.
- [3] Y. Zhang, K. Zhang, J. Wang, Z. Tian, A. D. Q. Li, *Nanoscale* **2015**, *7*, 19342.
- [4] J. Zhang, J. Wang, H. Tian, *Mater. Horiz.* **2014**, *1*, 169.
- [5] J. Zhang, Q. Zou, H. Tian, *Adv. Mater.* **2013**, *25*, 378.
- [6] M.-M. Russew, S. Hecht, *Adv. Mater.* **2010**, *22*, 3348.
- [7] M. Berberich, A.-M. Krause, M. Orlandi, F. Scandola, F. Würthner, *Angew. Chem., Int. Ed.* **2008**, *47*, 6616.
- [8] H. Wu, Y. Chen, Y. Liu, *Adv. Mater.* **2017**, *29*, 1605271.
- [9] U. Pischel, *Angew. Chem., Int. Ed.* **2007**, *46*, 4026.
- [10] A. Seeboth, D. Löttsch, R. Ruhmann, O. Muehling, *Chem. Rev.* **2014**, *114*, 3037.
- [11] A. Julià López, D. Ruiz-Molina, K. Landfester, M. B. Bannwarth, C. Roscini, *Adv. Funct. Mater.* **2018**, *28*, 1801492.
- [12] X. Wang, O. S. Wolfbeis, R. J. Meier, *Chem. Soc. Rev.* **2013**, *42*, 7834.
- [13] J. Zhou, B. del Rosal, D. Jaque, S. Uchiyama, D. Jin, *Nat. Methods* **2020**, *17*, 967.
- [14] W. Ren, G. Lin, C. Clarke, J. Zhou, D. Jin, *Adv. Mater.* **2020**, *32*, 1901430.
- [15] M. Sauer, *Proc. Natl. Acad. Sci. U. S. A.* **2005**, *102*, 9433.
- [16] M. Li, J. Zhao, H. Chu, Y. Mi, Z. Zhou, Z. Di, M. Zhao, L. Li, *Adv. Mater.* **2018**, *31*, 1804745.
- [17] D. Kim, K. Jeong, J. E. Kwon, H. Park, S. Lee, S. Kim, S. Y. Park, *Nat. Commun.* **2019**, *10*, 3089.
- [18] A. Abdollahi, H. Roghani-Mamaqani, B. Razavi, M. Salami-Kalajahi, *ACS Nano* **2020**, *14*, 14417.
- [19] Q. Qi, C. Li, X. Liu, S. Jiang, Z. Xu, R. Lee, M. Zhu, B. Xu, W. Tian, *J. Am. Chem. Soc.* **2017**, *139*, 16036.
- [20] Y. Ma, Y. Dong, S. Liu, P. She, J. Lu, S. Liu, W. Huang, Q. Zhao, *Adv. Opt. Mater.* **2020**, *8*, 1901687.
- [21] A. Kishimura, T. Yamashita, K. Yamaguchi, T. Aida, *Nat. Mater.* **2005**, *4*, 546.
- [22] D. Kim, S. Y. Park, *Adv. Opt. Mater.* **2018**, *6*, 1800678.
- [23] B. Daly, J. Linga, A. P. de Silva, *Chem. Soc. Rev.* **2015**, *44*, 4203.
- [24] K. P. Carter, A. M. Young, A. E. Palmer, *Chem. Rev.* **2014**, *114*, 4564.
- [25] E. Betzig, G. H. Patterson, R. Sougrat, O. W. Lindwasser, S. Olenych, J. S. Bonifacio, M. W. Davidson, J. Lippincot-Schwartz, H. F. Hess, *Science* **2006**, *313*, 1642.
- [26] M. Heilemann, S. van de Linde, M. Schüttelpe, R. Kasper, B. Seefeldt, A. Mukherjee, P. Tinnefeld, M. Sauer, *Angew. Chem., Int. Ed.* **2008**, *47*, 6172.
- [27] T. Grotjohann, I. Testa, M. Leutenegger, H. Bock, N. T. Urban, F. Lavoie-Cardinal, K. I. Willig, C. Eggeling, S. Jakobs, S. W. Hell, *Nature* **2011**, *478*, 204.
- [28] B. Roubinet, M. L. Bossi, P. Alt, M. Leutenegger, H. Shojaei, S. Schnorrenberg, S. Nizamov, M. Irie, V. N. Belov, S. W. Hell, *Angew. Chem., Int. Ed.* **2016**, *55*, 15429.
- [29] S.-H. Park, N. Kwon, J.-H. Lee, J. Yoon, I. Shin, *Chem. Soc. Rev.* **2020**, *49*, 143.
- [30] F. M. Raymo, M. Tomasulo, *Chem. Soc. Rev.* **2005**, *34*, 327.
- [31] J. R. Otaegui, P. Rubirola, D. Ruiz-Molina, J. Hernando, C. Roscini, *Adv. Opt. Mater.* **2020**, *8*, 2001063.
- [32] J. Otaegui, D. Ruiz-Molina, L. Latterini, C. Roscini, J. Hernando, *Mater. Horiz.* **2021**, *8*, 3043.
- [33] G. Massaro, J. Hernando, D. Ruiz-Molina, C. Roscini, L. Latterini, *Chem. Mater.* **2016**, *28*, 738.
- [34] G. Massaro, G. Zampini, D. Ruiz-Molina, J. Hernando, C. Roscini, L. Latterini, *J. Phys. Chem. C* **2019**, *123*, 4632.
- [35] W. Zhang, X. Ji, B. Peng, S. Che, F. Ge, W. Liu, M. Al-Hashimi, C. Wang, L. Fang, *Adv. Funct. Mater.* **2020**, *30*, 1906463.
- [36] J. Du, L. Sheng, Q. Chen, Y. Xu, W. Li, X. Wang, M. Li, S. X. Zhang, *Mater. Horiz.* **2019**, *6*, 1654.
- [37] Y. J. Jin, R. Dogra, I. W. Cheong, G. Kwak, *ACS Appl. Mater. Interfaces* **2015**, *7*, 14485.
- [38] J. Du, L. Sheng, Y. Xu, Q. Chen, C. Gu, M. Li, S. X.-A. Zhang, *Adv. Mater.* **2021**, *33*, 2008055.
- [39] H. Liu, W. Song, X. Chen, J. Mei, Z. Zhang, J. Su, *Mater. Chem. Front.* **2021**, *5*, 2294.
- [40] R. Liao, S. Gu, X. Wang, X. Zhang, X. Xie, H. Sun, W. Huang, *J. Mater. Chem. C* **2020**, *8*, 8430.
- [41] F. Würthner, *Chem. Commun.* **2004**, 1564.
- [42] L. Parejo, M. Chaari, S. Santiago, G. Guirado, F. Teixidor, R. Núñez, J. Hernando, *Chem. - Eur. J.* **2021**, *27*, 270.
- [43] K. Trofymchuk, A. Reisch, I. Shulov, Y. Mély, A. S. Klymchenko, *Nanoscale* **2014**, *6*, 12934.
- [44] W. Haynes, *CRC Handbook of Chemistry and Physics*, CRC Press, Boca Raton, FL **2014**.